Planar Inverted-F Antenna Design for a Fully Implantable Mechanical Circulatory Support System

Planar Inverted-F Antenna Design for a Fully Implantable Mechanical Circulatory Support System

Oliver Knecht, Yves Jundt and Johann W. Kolar
Power Electronic Systems Laboratory, ETH Zürich, Switzerland, e-mail: knecht@lem.ee.ethz.ch

***Abstract*— Transcutaneous Energy Transfer (TET) is a promising solution to operate implantable mechanical blood pumps such as Left Ventricular Assist Devices (LVAD) without the need for a percutaneous driveline. In order to control the power flow of the wireless energy transfer system and in order to transmit sensor data, a wireless communication channel is needed. This paper describes the design of an implantable Planar Inverted-F Antenna (PIFA) for the use with a TET system, which operates in the MedRadio band at 403.5 MHz and which is suitable for implantation depths of more than 20 mm. The focus of this work is on the practical implementation of the antenna, and the critical design parameters as well as the influence of the human tissue on the antenna design are discussed in detail. Finally, the antenna is built in hardware and the electrical characteristics of the antenna are measured using a muscle tissue mimicking liquid solution. The implemented antenna achieves nearly perfect impedance matching at 403.5 MHz with a return loss of more than 25 dB and a high gain of -26.3 dBi, even for a placement as deep as 20 mm within the tissue mimicking liquid. Numerical simulations further show that a maximum spatial-average SAR of 0.27 W/kg is achieved in the muscle model with the maximum allowed antenna input power of 9.35 dBm, which is a factor of six below the most stringent SAR limit of 1.6 W/kg.**

***Index Terms*—Wireless communication, PIFA, antenna design, active medical implant**

I. Introduction

In industrialized nations, the growing number of people suffering from end stage heart failure promoted the development of Mechanical Circulatory Support Systems (MCSS), which includes an implantable mechanical blood pump, such as a Left Ventricular Assist Device (LVAD), in order to support the weakened heart. Today, these devices are powered by means of a percutaneous driveline which penetrates the skin permanently and therefore represents a severe risk of infection to the patient. In order to eliminate the need for a galvanic contact, an Inductive Power Transfer (IPT) system was designed in [1], which is the key part in a Transcutaneous Energy Transfer (TET) system, as illustrated in **Fig. 1**. The TET system consists of a primary side main battery power supply, the IPT system and an implanted backup battery storage and its charging circuit. In addition, a motor inverter is implanted to operate the LVAD. In order to control the terminal voltage on the secondary side of the IPT system, a wireless communication channel is needed. In addition, the communication channel should be accessible for the transmission of sensor and control data in order to supervise and control the LVAD operation.

There are two main possibilities for establishing a wireless communication between the implanted and extracorporeal part of the TET system. The first method is to use the inductive power transfer coils for the information transfer by means of an amplitude modulation of the transmitted power using a Load Shift Keying (LSK) modulation scheme or by modulating the resonance frequency of the IPT resonant tank [2]–[4]. This method has the disadvantage that the information transfer is possible only if the power transmitter is in operation and is located in close proximity to the power receiver coil. Another disadvantage is the limited achievable bandwidth of the communication channel due to the relatively low frequency of the carrier signal of a few hundreds of kilohertz.

The second possibility for the implementation of the wireless communication channel is to use separate high-frequency transceivers including antennas on the primary and secondary side. The main advantage of this type of communication system is the ease of use, using highly integrated off-the-shelf radio frequency transceivers, which allow to implement a reliable bidirectional communication link with data rates up to 1 Mbps using Frequency Shift Keying (FSK) modulation schemes. Therefore, this type of communication system is considered the most suitable solution for the transmission of control and sensor data and remote monitoring of the implanted blood pump. However, the design of the implantable antenna, which is the main topic of this paper, poses several design challenges, as the antenna must be able operate in the electromagnetically hostile environment of the human body.

Implantable active devices such as cardiac pacemakers and defibrillators are allowed to communicate in dedicated frequency bands, such as the Medical Implant Communication Service (MICS), which was established by the Federal Communications Commission (FCC) in 1999 and covers the frequency range of 402-405 MHz. In 2009, the FCC extended the frequency range to 401-406 MHz, which is known today as the Medical Device Radiocommunications Service (MedRadio), and added 24 MHz of additional spectrum to the MedRadio band in the frequency range of 413-457 MHz in 2011 [5]. The distribution of the MedRadio band between 400 MHz and 500 MHz is illustrated in **Fig. 2**.

The implantable antenna described in this paper is designed for an operation within the MICS band at a center frequency of 403.5 MHz. The maximum radiated power within the MICS band is limited to a low maximum Equivalent Isotropically Radiated Power (EIRP) of -16 dBm (25 μW) [6], in order to minimize the risk of interference with other medical devices operating in the same frequency range. Further, the maximum authorized bandwidth within the frequency band is 300 kHz. If a higher bandwidth is required, the antenna design could be adapted easily to operate at a higher frequency, e.g. in between 413-419 MHz, where the authorized bandwidth is specified with 6 MHz.

In **Section II**, the antenna design and the influence of the

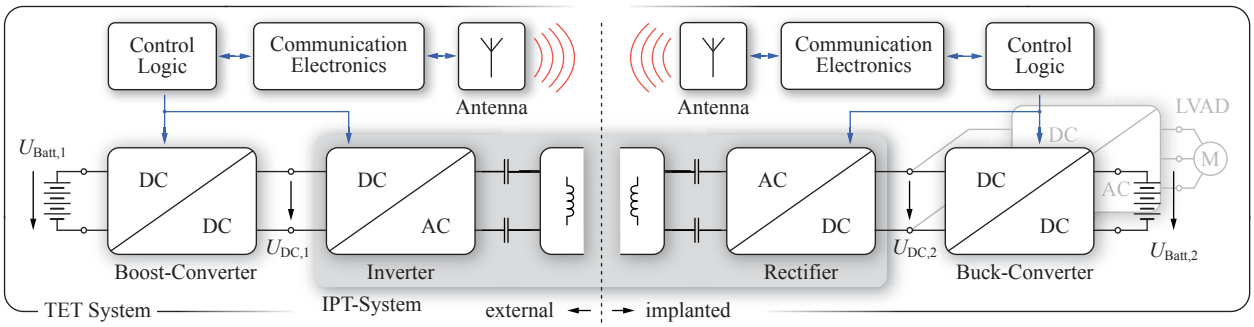

Figure 1: Schematic concept of the Transcutaneous Energy Transfer (TET) system.

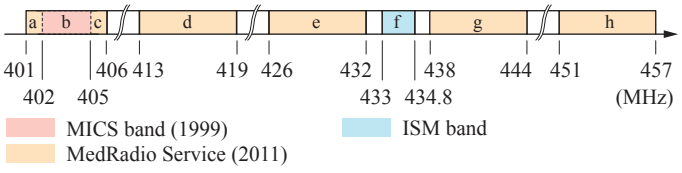

Frequency Band (MHz)	Authorized Bandwidth (kHz)	Frequency Band (MHz)	Authorized Bandwidth (kHz)
a) 401 - 401.85	100	e) 426 - 432	6000
401.85 - 402	150	f) 433.05 - 434.79	ISM band
b) 402 - 405	300	g) 438 - 444	6000
c) 405 - 406	100	h) 451 - 457	6000
d) 413 - 419	6000		

Figure 2: Medical Device Radiocommunications Service (MedRadio) frequency spectrum overview and authorized bandwidths [5].

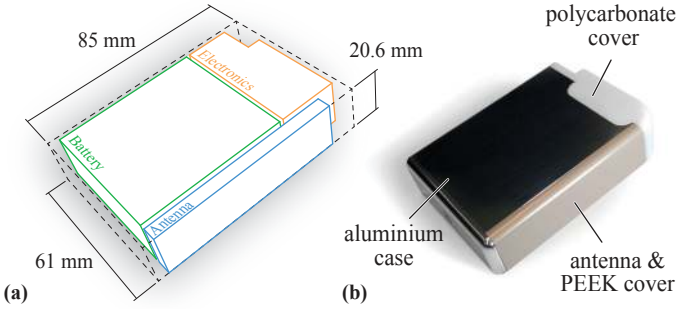

Figure 3: (a) Distribution and space occupation of the main implanted electrical components, i.e. the backup battery, the power and control electronic components and the antenna. (b) Implant dummy enclosure and integrated antenna assembly, which was used for the in-vitro measurements.

human tissue on the antenna characteristics are discussed. The optimized antenna design was then build in hardware and is presented in the same section. In a next step, the antenna characteristics such as return loss and antenna gain are measured using a tissue mimicking liquid. The measurement results are then compared to the numerical simulation and are presented in **Section III**. In **Section IV**, the exposure of the tissue model to the electromagnetic field is assessed according to the regulations on Specific Absorption Rate (SAR), using a numerical simulation. Concluding remarks are given in **Section V**

II. Antenna Design

A main objective of the design of implantable antennas is to minimize the antenna volume. However, the allowed volume occupation of the antenna is highly dependent on the actual implant dimensions and design. In order to maximize the antenna performance, i.e. gain and radiation efficiency, the antenna should be built using the maximum space available that is feasible for the implant at hand. **Fig. 3(a)** illustrates the allocation of the electronic components and its volume occupation for the preliminary design of the implantable part of the TET system. The boxed volume of the implant is 10.7 cl, and is mainly determined by the backup battery, which occupies the largest amount of volume and which defines the overall thickness of the implant. The antenna is placed on the side of the enclosure, such that the implant can be built as thin as possible, while offering a large surface area of 69 mm×20.6 mm for the antenna design. The total height of the antenna assembly, including the superstrate material is 5 mm. Hence, the total boxed volume of the antenna is 6.65 cl, which accounts for 6.2 % of the total implant volume.

In [7], [8] it was shown that magnetic dipoles, i.e. loop antennas, offer higher radiation efficiencies than electric sources such as a patch antenna or the electric dipole antenna, when operated within the human body. The human tissue is non-magnetic and barely interacts with the magnetic field. Hence, the strong magnetic near field is not absorbed. However, placing a loop antenna near to the surface of the metallic enclosure of the implant, increases the power losses and disturbs the magnetic field significantly. Therefore, it was decided to chose the Planar Inverted-F Antenna (PIFA) for the antenna implementation, which benefits from the large reference ground plane formed by the implant enclosure, which in turn shields the internal electronics from the electromagnetic field generated by the antenna. Furthermore, the PIFA offers a highly compact design with a low profile and offers higher radiation efficiency within the human body when compared to conventional microstrip antennas (e.g. spiral-type microstrip antennas), as it was shown in [9].

Following the design guidelines reported in [7], the antenna was first designed in air in order to reveal the critical geometric design parameters and in a second step, the lossy tissue material is added to the model and the previously found design parameters are then used to optimize the antenna with the objective to maximize the input impedance matching, the antenna gain and the radiation efficiency.

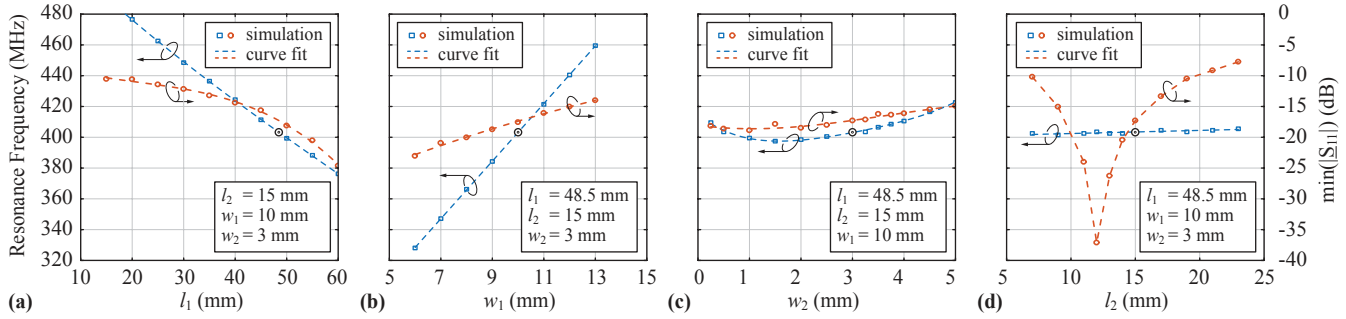

Figure 4: Influence of the variation of the main patch design parameter l_1, l_2, w_1 and w_2 on the resonance frequency and input impedance matching of the antenna.

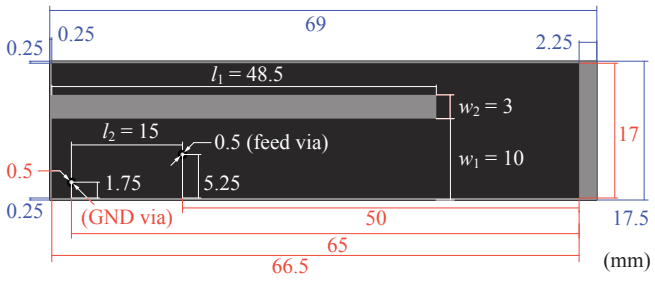

Figure 5: PIFA patch and substrate dimensions.

In the following sections, the influence of the geometric design, the antenna substrate and superstrate material, as well as the influence of the human tissue on the antenna performance are discussed.

A. *PIFA Patch Design*

The numerical simulations are performed using the Ansys High Frequency Structure Simulator (HFSS). In [10], it was shown that the size of the PIFA's ground plane has a significant influence on the bandwidth, the radiation pattern and the achieved gain of the antenna. Therefore, the antenna assembly is simulated together with the implant case, which is modelled as solid block of aluminium with a polycarbonate top cover. The ground plane of the PIFA is electrically connected to the implant enclosure and is thereby increased in size. As a result, the radiation pattern is altered and the gain of the antenna is increased significantly.

The geometry and the dimensioning of the final PIFA patch is shown in **Fig. 5**. According to the findings provided in [10], the PIFA patch size is maximized and the via connection to the ground plane is placed in the corner of the ground plane's short edge in order to enhance the antenna performance, i.e. the antenna gain and the fractional bandwidth. Due to the large quarter wavelength at the target frequency of 403.5 MHz, a slot is introduced in the patch design to increase the electrical length of the antenna and hence, to reduce its resonance frequency.

The main geometric design parameters used to tune and optimize the antenna characteristics are labeled with l_1, l_2, w_1 and w_2, as shown in **Fig. 5**. The influence of these parameters on the resonance frequency and the input impedance matching of the antenna are shown in **Fig. 4(a)-(d)** for the final antenna geometry, simulated within the lossy tissue. As shown in **Fig. 4(a)** and **(b)**, the resonance frequency of the antenna is mainly determined by the parameters l_1 and w_1. As the length of the slot l_1 is increased, the resonance frequency is decreasing linearly due the increase of the electrical length of the antenna. A similar effect can be observed with the variation of the distance w_1. By moving the slot further away from the ground via, the current density on the long edge of the patch, opposite to the ground via, is decreasing and hence, the effective electrical length of the patch is decreased as well. Note that the tuning of l_1 and w_1 do also have a significant influence on the impedance matching of the antenna.

The width of the slot, denoted with w_2, has a less prominent influence on the resonance frequency and on the impedance matching of the antenna and can be used for fine-tuning, as shown in **Fig. 4(c)**. As the width of the slot is increased, the resonance frequency rises because of the increasing impedance of the delimited part of the patch, which in turn decreases the effective electrical length of the antenna. On the other hand, if the slot width is much smaller than the thickness of the substrate, the capacitive coupling between the separated parts of the patch becomes dominant and the resonant frequency rises again since the slot loses its effectiveness.

As explained above, the parameter l_1, w_1 and w_2 are used to tune the antenna for an operation at the desired resonant frequency. Then, in a second step, the distance l_2 between the ground via and the feed-point via is used to tune the antenna's input impedance, as shown in **Fig. 4(d)**.

Hence, a good knowledge of the influence of the geometric degrees of freedom on the main antenna characteristics is the basis for an optimization of the antenna, or for an adaptation of the antenna to different substrate and superstrate materials and different human tissues.

B. *PIFA Substrate*

The substrate material properties and layer thickness have a significant influence on the resonance frequency, radiation efficiency and fractional bandwidth of the antenna [11]–[13]. A substrate material with high relative permittivity increases the electrical length of the antenna, which decreases the resonance frequency and hence allows for a more compact design of the antenna, but the bandwidth of the antenna decreases as well, because the quality factor of the antenna is increased. The bandwidth of the antenna can be enhanced by increasing the height of the substrate, as reported in [11], [13]. But considering the specified total height of 5 mm of the antenna assembly, a

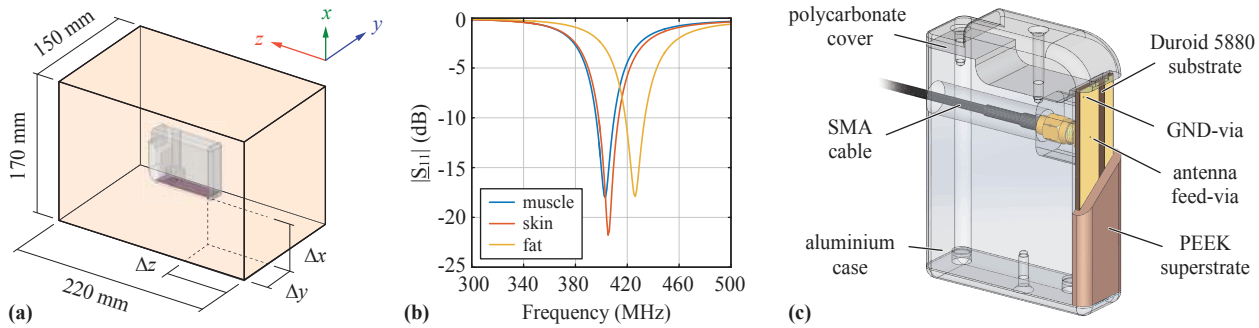

Figure 6: (a) Dimensions of the muscle tissue model used for the numerical simulation and location of the implant within the tissue. (b) Influence of common human tissues on the resonance frequency of the final antenna design. (c) Schematic drawing of the hardware design of the final antenna assembly and the dummy implant used for the experimental verification.

Parameter	Muscle	Skin	Fat
Relative Permittivity†	57.1	46.7	11.6
El. Conductiviy (S/m)†	0.797	0.69	0.08
Density (kg/m^3)	1090	1109	911

†evaluated at $f = 403.5$ MHz.

Table I: Dielectric properties and densities of selected human tissues [14].

thicker substrate comes at the expense of a reduced superstrate thickness which is not preferred, as pointed out in the following section.

Following these considerations and given the large area available for the antenna design, a substrate material with low permittivity and low profile is used. In addition, a material with a low dissipation factor is preferred in order to minimize the power loss in the substrate. Therefore, the substrate material Duroid 5880 was used with a standardized thickness of 1.575 mm. The relative permittivity of this material is $\varepsilon_\mathrm{r} = 2.2$ and the dissipation factor is as low as $\tan(\delta) = 0.0004{-}0.0009$, which allows to enhance the efficiency of the antenna significantly.

C. PIFA Superstrate

The superstrate of the antenna has a particularly important role in the design of implantable antennas. The superstrate layer insulates the antenna patch from the electrically conductive human tissue and furthermore, it acts as a buffer layer that allows to confine the high electrical near field component within the superstrate layer, due to the much higher permittivity of the biological tissue compared to the insulation layer. Hence, the power loss in the biological tissue can be reduced, which in turn improves the radiation efficiency of the antenna, as described in detail in [7], [15], [16]. Concerning the material permittivity, numerical simulations with the antenna design at hand showed, that an increase of the permittivity of the superstrate material is not advantageous as it results in higher tissue power losses and therefore in a reduced radiation efficiency. Hence, a thick layer of low-loss superstrate material with low permittivity is preferred. For the application at hand, PEEK (polyetheretherketone) is used as insulation material, which has a relative permittivity of $\varepsilon_\mathrm{r} = 3.2$ and a dissipation factor of $\tan(\delta) = 0.003$ [17]. As pointed out in [7], PEEK is not the optimal solution to maximize the performance of the antenna, but it offers excellent mechanical properties and it is a biocompatible material, which is widely accepted for the use in medical implants [18].

D. Influence of Human Tissue

In this study a simple homogeneous muscle tissue model was used for the simulations, and hence, a muscle tissue mimicking liquid was used for the in-vitro measurements in order to verify the simulation results, as described in **Section III**. The dimensions of the simulation model are shown in **Fig. 6(a)** and the antenna substrate is positioned at the location $\Delta x = 77.5\,\mathrm{mm}$, $\Delta y = 21.5\,\mathrm{mm}$ and $\Delta z = 52\,\mathrm{mm}$. Due to the high relative permittivity of the human tissue, the resonance frequency is decreased significantly, which allows to further reduce the size of the antenna or to choose a substrate and superstrate material with lower permittivity and therefore, enhancing the fractional bandwidth of the antenna. The influence of replacing the tissue volume with muscle, fat or skin tissue on the resonance frequency is shown in **Fig. 6(b)** and the dielectric properties of the considered tissues are summarized in **Tab. I** for the design frequency of 403.5 MHz [14]. From **Fig. 6(b)** it can be seen that the composition of the tissue in close proximity of the antenna has a significant influence on the resonance frequency. A high fat content in the tissue surrounding the antenna shifts the resonance frequency towards higher frequencies due to its low permittivity. Therefore, the actual location of the implant in the human body needs to be known for the final tuning of the antenna.

E. Hardware Prototype

Fig. 6(c) shows a schematic drawing of the hardware prototype of the antenna assembly and the dummy implant. The PEEK superstrate covers the entire PIFA and has a thickness of 3.425 mm at the surface of the antenna patch. The ground plane of the antenna is electrically connected to the solid aluminium implant dummy which provides a feed-through for the supply cable that is connected to the antenna feed-point. The top cover of the dummy implant, which represents the connector block for the connection of the TET coil and the driveline of the LVAD, is manufactured from polycarbonate. The final fabricated hardware assembly, which was used for experimental verification, is shown in **Fig. 3(b)**.

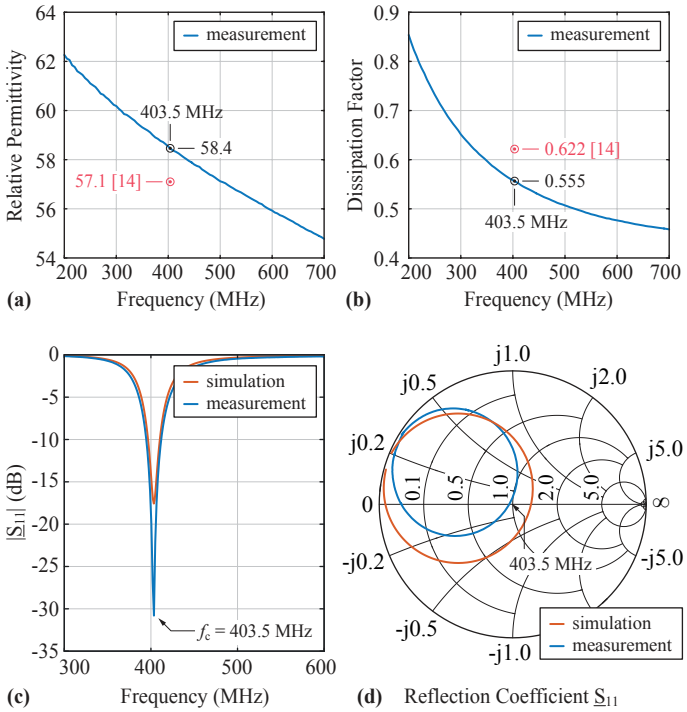

Figure 7: Measurement of the relative permittivity (a) and the dissipation factor (b) of the muscle mimicking liquid. (c)-(d) comparison of the measured and simulated reflection coefficient $\underline{S}_{11}$.

III. Experimental Verification

For the measurement of the resonance frequency, the input impedance matching and the radiation pattern of the antenna, the implant dummy was immersed in a muscle tissue mimicking liquid with a total volume of 5.6 l and the same dimensions as the simulation model shown in **Fig. 6(a)**. For the manufacturing of the muscle tissue mimicking liquid, the recipe provided in [7] was used, which contains 51.3 % (weight percentage) de-ionised water, 47.3 % sugar and 1.4 % pure NaCl (sodium chloride). At a temperature of 22 °C, the liquid solution exhibits dielectric properties equivalent to living muscle tissue at a frequency of 403.5 MHz and a temperature of 37 °C. The relative permittivity and the dissipation factor are measured using a HP (Keysight) 85070B dielectric probe kit and the results are shown in **Fig. 7(a)-(b)**. The relative error of the measured relative permittivity with respect to the value provided by [14] is 2.3 % and -10.8 % for the dissipation factor.

Parameter	Simulation	Measurement
Resonance Frequency	403.3 MHz	403.5 MHz
Max. Return Loss	17.5 dB	30.8 dB
Matching Bandwidth	13.0 MHz	17.3 MHz
Antenna Gain†	-27.9 dBi	-26.3 dBi
Radiation Efficiency	0.135 %	—

†antenna gain in the direction towards 180°, out of the muscle mimicking liquid, as defined in Fig. 8(a).

Table II: Summary of the simulated and measured antenna parameter.

The measured and simulated reflection coefficient at the feed-point of the antenna is shown in **Fig. 7(c)** and **(d)**. The resonance frequency of the realized antenna is exactly 403.5 MHz and a return loss of more than 25 dB was achieved at the center frequency. The impedance matching bandwidth at a return loss of 10 dB is 17.3 MHz, which is much larger than the bandwidth needed for this application.

The gain of the antenna was measured with the orientation and placement of the dummy implant as shown in **Fig. 6(a)**. As reference antenna, a wideband logarithmic-periodic antenna with a gain of 5 dBi was used and was located on the same level at a free-space distance of 4.1 m from the antenna test setup, as indicated in **Fig. 8(a)**. The gain of the implantable antenna was measured in the direction of vertical polarisation, i.e. with the reference antenna polarization oriented in the x-direction, and in the direction of horizontal polarisation, i.e. with the reference antenna polarization oriented in z-direction.

The results of the gain measurements are shown in **Fig. 8(b)** and **(c)**. The measured radiation pattern in the direction of vertical polarization is in good agreement with the simulated values. In this case, the measured antenna gain in the direction towards 180°, out of the muscle mimicking liquid, attains a value of -26.3 dBi, despite the large 'implantation depth' of 20 mm. The gain in the direction of horizontal polarisation is much lower compared to the vertical polarization, which was expected, considering the planar structure of the PIFA.

The simulated and measured performance characteristics of the realized PIFA operated in the muscle mimicking liquid are summarized in **Tab. II**. The simulated peak gain attains a value of -25.35 dBi and the peak directivity is 3.33 dBi. Hence, the radiation efficiency of the antenna attains a value of 0.135 %,

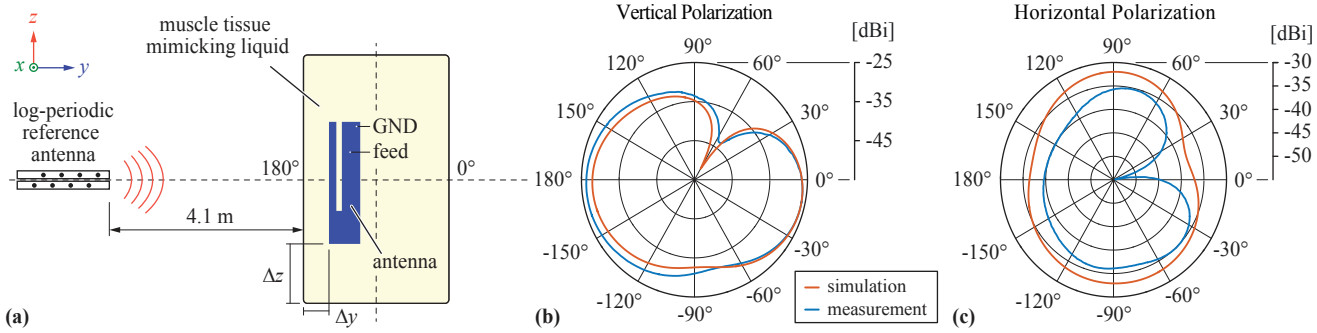

Figure 8: (a) Measurement setup and orientation of the antenna used for the gain measurement in the anechoic chamber. (b)-(c) In-vitro measurement of the antenna gain in the y-z-plane for vertical polarisation (i.e. in x-direction) and horizontal polarization (i.e in z-direction) of the antenna.

which is mainly limited by the high power loss caused by the tissue material surrounding the implant.

IV. Exposure Assessment

The exposure of the human body to time-varying electromagnetic fields in the megahertz range is generally assessed in terms of Specific Absorption Rate (SAR), which is a measure of the absorbed power per mass of tissue, expressed in watts per kilogram. Typically, for local SAR assessment, the spatial-average SAR is used, defined as the average of the local peak SAR over a predefined tissue volume [19]. The limits for general public exposure are defined in [19] and [20] as 2 W/kg for 10 g averaging volume and as 1.6 W/kg for the 1 g average [21]. With the simple muscle tissue model used in this study a power of 17.1 dBm (51 mW) could be supplied at the antenna input terminal in order to comply with the 1.6 W/kg (1 g average) SAR limit. However, in order to comply with the maximum allowed equivalent isotropically radiated power of -16 dBm specified in [6], and considering the simulated peak gain of -25.35 dBi, a maximum power of 9.35 dBm (8.6 mW) could be supplied at the antenna input. This results in a maximum spatial-average SAR of 0.27 W/kg, which is a factor of six below the most stringent SAR limit. As pointed out in [7], for a final exposure assessment, a detailed heterogeneous human body model needs to be considered, which will be a topic of future work.

V. Conclusions

In this paper, the practical design and characterization of an implantable antenna for a TET system is shown. The design approach and the critical design considerations are described in detail, and are generally applicable. It is important to note, that the antenna must be designed and optimized for the specific application, considering the actual material and dimensions of the implant enclosure. Further, the antenna volume should be maximized within the limits given by the implant design in order to enhance the gain and the radiation efficiency of the antenna. An important design parameter is the material and the thickness of the superstrate. A thick superstrate with low permittivity is preferred in order to confine the high electric near field of the antenna in the insulation layer, which decreases the power losses in the tissue significantly. Hence, given the volume of the PIFA assembly, the substrate thickness should be reduced and a low permittivity substrate material should be used in order to enhance the bandwidth of the antenna.

The final antenna prototype is designed for an operation at 403.5 MHz and achieves a gain of -26.3 dBi, even when immersed in the lossy muscle tissue mimicking liquid in a depth of 20 mm from the surface. With the simple tissue model at hand, the numerical simulation show that the antenna design complies with the regulations on SAR. Future work includes the fine tuning of the antenna design according to the tissue properties at the final implant location and the exposure assessment using a more detailed human body model.

Acknowledgment

The authors gratefully acknowledge the financial support by the Baugarten foundation. Further thanks goes to Hans-Rudolf Benedickter and Martin Lanz for the help with the manufacturing and performance measurement of the antenna. This work is part of the Zurich Heart project under the umbrella of "University Medicine Zurich/Hochschulmedizin Zürich".

References

[1] O. Knecht, R. Bosshard, and J. W. Kolar, "High-efficiency transcutaneous energy transfer for implantable mechanical heart support systems," *IEEE Trans. Power Electron.*, vol. 30, no. 11, pp. 6221–6236, 2015.

[2] X. Shi, A. N. Parks, B. H. Waters, and J. R. Smith, "Co-optimization of efficiency and load modulation data rate in a wireless power transfer system," in *Proc. of the IEEE Int. Symp. on Circuits and Systems (ISCAS)*, 2015, pp. 698–701.

[3] S. Mandal and R. Sarpeshkar, "Power-efficient impedance-modulation wireless data links for biomedical implants," *IEEE Trans. Biomed. Circuits Syst.*, vol. 2, no. 4, pp. 301–315, 2008.

[4] G. Yilmaz and C. Dehollain, "Capacitive detuning optimization for wireless uplink communication in neural implants," in *Proc. of the 5th IEEE Int. Workshop on Advances in Sensors and Interfaces (IWASI)*, 2013, pp. 45–50.

[5] Federal Communications Commission (FCC), "Medical Device Radiocommunications Service (MedRadio)," [Online]. Available: www.fcc.gov/general/medical-device-radiocommunications-service-medradio. [Accessed: Sept. 28, 2016].

[6] ——, "Amendment of Parts 2 and 95 of the Commission's Rules to Provide Additional Spectrum for the Medical Device Radiocommunication Service in the 413-457 MHz band". FCC 11-176, Washington, D.C., USA, Nov. 2011.

[7] F. Merli, "Implantable antennas for biomedical applications," Ph.D. dissertation, Dept. Elect. Eng., Swiss Federal Inst. Technol. Lausanne (EPFL), Lausanne, Switzerland, 2011.

[8] A. Karlsson, "Physical limitations of antennas in a lossy medium," *IEEE Trans. Antennas Propag.*, vol. 52, no. 8, pp. 2027–2033, 2004.

[9] J. Kim and Y. Rahmat-Samii, "Implanted antennas inside a human body: simulations, designs, and characterizations," *IEEE Trans. Microw. Theory Techn.*, vol. 52, no. 8, pp. 1934–1943, 2004.

[10] M. C. Huynh and W. Stutzman, "Ground plane effects on planar inverted-F antenna (PIFA) performance," *IEE Proc. - Microw. Antennas and Propag.*, vol. 150, no. 4, pp. 209–213, 2003.

[11] H. T. Chattha, Y. Huang, M. K. Ishfaq, and S. J. Boyes, "A comprehensive parametric study of planar inverted-F antenna," *Wireless Engineering and Technology*, vol. 3, no. 1, pp. 1–11, 2012.

[12] Y. T. Jean-Charles, V. Ungvichian, and J. A. Barbosa, "Effects of substrate permittivity on planar inverted-F antenna performances," *Journal of Computers*, vol. 4, no. 7, pp. 610–614, 2009.

[13] P. Soontornpipit, C. M. Furse, and Y. C. Chung, "Design of implantable microstrip antenna for communication with medical implants," *IEEE Trans. Microw. Theory Techn.*, vol. 52, no. 8, pp. 1944–1951, 2004.

[14] Foundation for Research on Information Technology in Society (IT'IS), "Tissue Properties," [Online]. Available: www.itis.ethz.ch/virtual-population/tissue-properties/database. [Accessed: Oct. 07, 2016].

[15] A. Mahanfar, S. Bila, M. Aubourg, and S. Verdeyme, "Design considerations for the implanted antennas," in *Proc. of the IEEE/MTT-S Int. Microwave Symp.*, 2007, pp. 1353–1356.

[16] V. T. Nguyen and C. W. Jung, "Impact of dielectric constant on embedded antenna efficiency," *Int. J. Antennas Propag.*, vol. 2014, no. 1, pp. 1–6, 2014.

[17] Victrex, "VICTREX PEEK properties brochure (metric units)," [Online]. Available: www.victrex.com/~/media/literature/en/victrex_properties-guide_en_metric.pdf. [Accessed: 21.2.2017].

[18] S. M. Kurtz and J. N. Devine, "PEEK biomaterials in trauma, orthopedic, and spinal implants," *Biomaterials*, vol. 28, no. 32, pp. 4845–4869, 2007.

[19] Institute of Electrical and Electronics Engineers (IEEE), "IEEE standard for safety levels with respect to human exposure to radio frequency electromagnetic fields, 3 kHz to 300 GHz". IEEE Std C95.1-2005, New York, NY, USA, Apr. 2006.

[20] International Commission on Non-Ionizing Radiation Protection (ICNIRP), "Guidelines for limiting exposure to time-varying electric, magnetic and electromagnetic fields (up to 300 GHz)," *Health Phys.*, vol. 74, no. 4, pp. 494–522, 1998.

[21] Federal Communications Commission (FCC), "Guidelines for evaluating the environmental effects of radiofrequency radiation". FCC 96-326, Washington, D.C., USA, Aug. 1996.